International Journal of Microwave and Wireless Technologies

cambridge.org/mrf

Clutter removal for measuring low-frequency narrow-band antenna using spectral estimation

C. F. Hu and N. J. Li

Northwestern Polytechnical University, Youyi West Road, Xi'an, China

Research Paper

Cite this article: Hu CF, Li NJ (2019). Clutter removal for measuring low-frequency narrow-band antenna using spectral estimation. *International Journal of Microwave and Wireless Technologies* **11**, 215–219. https://doi.org/10.1017/S1759078718001241

Received: 23 October 2017
Revised: 1 August 2018
Accepted: 8 August 2018
First published online: 13 September 2018

Key words:
Antenna design; microwave measurements; modeling and measurements

Author for correspondence:
C. F. Hu, E-mail: huchufeng@nwpu.edu.cn

Abstract

The measurement accuracy of low-frequency narrow-band antenna is heavily influenced by its environment, which is also difficult to remove the clutter with a time gating. This paper proposes a method to improve the measurement accuracy of low-frequency narrow-band antenna using signal processing technique. The method is to predict the unknown value out of received original signal with an auto-regressive model (AR model) based on modern spectral estimation theory, and the parameters in AR model are calculated by maximum entropy spectral estimation algorithm. Thus, a wideband signal compared with the original band is obtained, and then the time-domain resolution is enhanced. The time gating is more exactly to separate the antenna radiation signal from multipath signals. The simulation and experimental results show that about 50% extended data for each ends of original band can be obtained after spectral extrapolation, and the time-domain resolution after extrapolation is twice than the original narrow-band signal, and the influence of measurement environment can be eliminated effectively. The method can be used to improve accuracy in actual antenna measurement.

Introduction

Low-frequency narrow-band antennas are widely used in communication and navigation systems for both manned and unmanned aircrafts, such as very high frequency (VHF) omnidirectional range (VOR), operating from 108 to 117.95 MHz, distance measuring equipment (DME), operating from 962 to 1213 MHz, and so on [1, 2]. For all these systems, the high precision measurement of antenna is very important.

As is well-known, the measurement of antenna radiation pattern at low frequency cannot be accurately performed in anechoic chambers because of their small size in terms of wavelength and poor absorption performance of their walls, and the multipath signal from the side wall and floor may influence measurement accuracy [3]. To remove the multipath signal of environment, many approaches are utilized [4–9]. The propagation of multipath signal has normally time lag compared with the antenna radiation signal, the separation of multipath signal with a time gating is an effective method [10]. Especially, the vector network analysis (VNA) is widely used, which can transmit stepped-frequency continuous waves and use the inverse fast Fourier transform (IFFT) to change the signal into time-domain response so as to remove clutter with the time gating [11]. However, when the band of a low-frequency antenna is narrow, and its equivalent time-domain resolution is relatively wide, thus being difficult to obtain the exact time gating to separate the main signal and multipath signal. Ref. [12] presented a technique named mathematical absorber reflection suppression (MARS) when the antenna measurement is performed in a non-ideal anechoic chamber. Ref. [13] developed an antenna measurement using an optical fiber link technique to suppress the reflection waves from the coaxial cable. Ref. [14] developed a method by utilizing the antenna's return lose to compensate for expanding the frequency band of the received signal, but the operation is a bit complex.

This paper proposes a signal processing technique to improve the measurement accuracy of a low-frequency narrow-band antenna. The method is to perform spectral extrapolation at the two ends of the original band using the Burg algorithm, namely to produce a wideband signal and thereby enhances the time-domain resolution. The time gating with the improved time-domain resolution can effectively eliminate multipath signal. 'Principle of method' section presents the principle and mathematical formulae of the method. 'Results' section gives the simulation results and the data of a low-frequency narrow-band antenna with a multipath signal measured in an anechoic chamber. The results show that the method is effective at improving the measurement accuracy of a low-frequency narrow-band antenna.

Principle of method

The principle of spectral extrapolation

In the antenna measurement with VNA, the relationship between equivalent time-domain resolution $d\tau$ and signal bandwidth BW is

$$d\tau = \frac{1}{BW}. \tag{1}$$

The corresponding range resolution Δd is

$$\Delta d = c \times d\tau = c/BW, \tag{2}$$

where c is the velocity of light.

As shown in Fig. 1, if the bandwidth is narrow, then the time-domain resolution and the corresponding range resolution are low, and thus it is difficult to distinguish between the main signal and multipath signals. The frequency domain data are extrapolated on both sides of the band according to the rule of statistics, and then a wideband signal can be obtained, so the time-domain resolution is improved. Based on the improved time-domain resolution, the multipath signal can be accurately separated by a time gating.

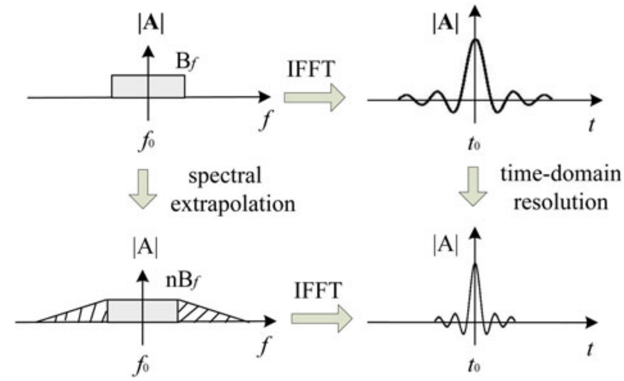

Fig. 1. The principle of spectral extrapolation.

The algorithm of spectral extrapolation

The spectral extrapolation method is based on the autoregressive model (AR model) in the modern spectral estimation theory. The model parameters are calculated by the Burg algorithm [15]. The core idea is: the period known correlation sequence is extrapolated to obtain the unknown value of the correlation sequence. The correlation function of sequence after extrapolation has the maximum entropy, which is to obtain maximum information of unknown spectrum. The AR model is a kind of linear prediction. For example, if the N points data are known, the data before or after N points can be predicted by the model, which is similar to the interpolation. The AR model is recursive by N points, and the interpolation is derived from two points (or a few points), both of them are to increase effective data. Since the predicted data have the same autocorrelation function as the known data, so the predicted data contain information of the known data. For a linear time-invariant system, its transfer function satisfies the AR model. While the indoor antenna testing can be viewed as a linearly time-invariant process, it is possible to predict before and after data by solving AR model parameters. The detailed formulae are as follows.

According to the definition of the AR model, the current data $x(n)$ can be represented by a linear combination of previous data $x(n-1)$, $x(n-2)$, …, $x(n-m)$:

$$x(n) = -\sum_{i=1}^{m} a_m(i)\, x(n-i) + e(n), \tag{3}$$

where $\hat{x}(n) = -\sum_{i=1}^{m} a_m(i)x(n-i)$ is the prediction data of $x(n)$, $e(n)$ is the prediction error, and $a_m(i)$is the coefficient of linear combination.

For the forward prediction, the prediction data $\hat{x}^f(n)$, the forward prediction error $e^f(n)$, and the forward prediction error power ρ^f are as follows:

$$\hat{x}^f(n) = -\sum_{i=1}^{m} a_m(i)x(n-i), \tag{4}$$

$$e^f(n) = x(n) - \hat{x}^f(n), \tag{5}$$

$$\rho^f = \frac{1}{N-m}\sum_{n=m}^{N-1} |e^f(n)|^2. \tag{6}$$

For the backward prediction, the prediction data $\hat{x}^b(n-m)$, the backward prediction error $e^b(n)$, and the backward prediction error power ρ^b are as follows:

$$\hat{x}^b(n-m) = -\sum_{i=1}^{m} a_m^*(i)x(n-m+i), \tag{7}$$

$$e^b(n) = x(n-m) - \hat{x}^b(n-m), \tag{8}$$

$$\rho^b = \frac{1}{N-m}\sum_{n=m}^{N-1} |e^b(n)|^2. \tag{9}$$

The coefficients $a_m(i)$ are calculated using the following recursion formulae:

$$a_m(i) = a_{m-1}(i) + k_m a_{m-1}^*(m-i), \tag{10}$$

$$a_m(m) = k_m, \tag{11}$$

where k_m is a recursion coefficient, and $i = 1, 2, \ldots, m-1$.

According to the recursion formulae, the relationships of $e^f(n)$ and $e^b(n)$ are given by the following formulae:

$$e_m^f(n) = e_{m-1}^f(n) + k_m e_{m-1}^b(n-1), \tag{12}$$

$$e_m^b(n) = e_{m-1}^b(n-1) + k_m^* e_{m-1}^f(n), \tag{13}$$

https://doi.org/10.1017/S1759078718001241 Published online by Cambridge University Press

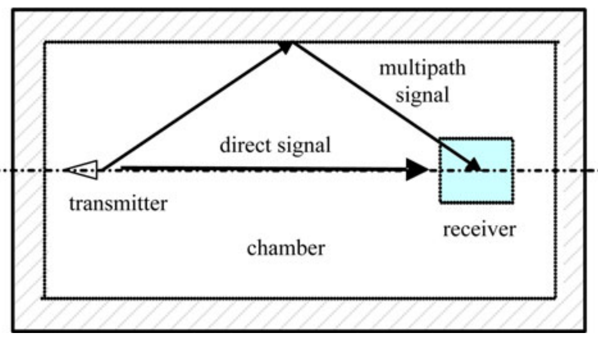

Fig. 2. The simulated signals in a non-ideal environment.

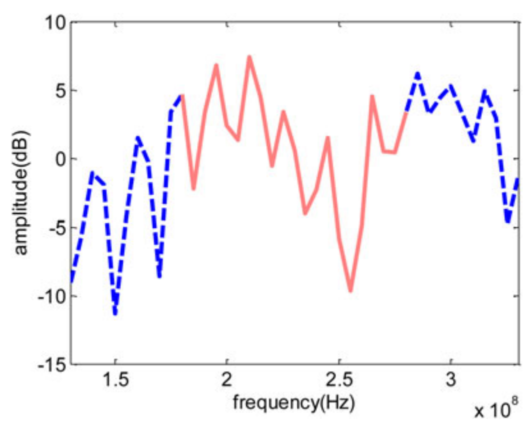

Fig. 3. The frequency domain signal before and after extrapolation.

$$e_0^f(n) = e_0^b(n) = x(n). \tag{14}$$

Let the sum of forward and backward prediction error powers is

$$\rho^{fb} = \frac{1}{2}[\rho^f + \rho^b]. \tag{15}$$

ρ^{fb} is only the function of k_m, and let $\partial\rho^{fb}/\partial k_m = 0$, we have

$$k_m = \frac{-2\sum_{n=m}^{N-1} e_{m-1}^f(n) e_{m-1}^{b*}(n-1)}{\sum_{n=m}^{N-1} |e_{m-1}^f(n)|^2 + \sum_{n=s}^{N-1} |e_{m-1}^b(n-1)|^2}, \tag{16}$$

where $m = 1, 2, \ldots, p$, and p is the model order.

The steps of obtaining extrapolated data using original data are as follows:

Step 1: Given the initial condition $e_0^f(n) = e_0^b(n) = x(n)$, then k_1 is estimated using (16);
Step 2: the model coefficient $a_1(1) = k_1$ is obtained for $m = 1$;
Step 3: $e_1^f(n)$ and $e_1^b(n)$ are obtained by k_1 and (12)–(14), then k_2 is estimated using (16);
Step 4: The model coefficients $a_2(1)$ and $a_2(2)$ for $m = 2$ are calculated using (10) and (11);
Step 5: Repeat steps 2–4 until $m = p$, all of model coefficients are obtained. Then the forward and backward prediction data can be calculated by the coefficients.

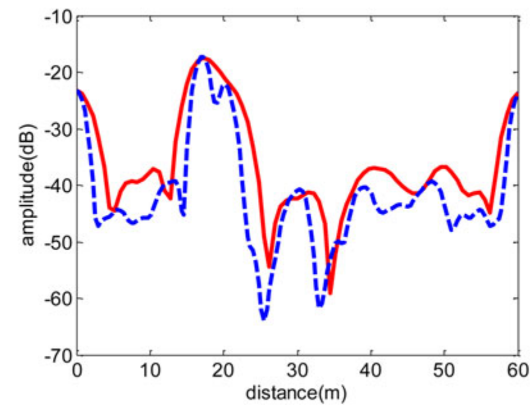

Fig. 4. The time-domain response before and after extrapolation.

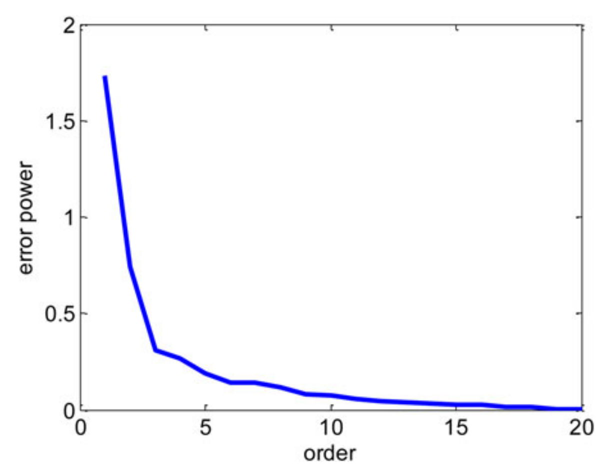

Fig. 5. The variation of error power with the model order.

Results

The simulation of method

The simulation data are generated in a non-ideal environment as shown in Fig. 2. The propagation distance of a direct signal is 17 m from the transmitter to the receiver; the propagation distance of a multipath signal caused by the wall is 20 m. The distance between two signals is 3 m. The amplitude of the multipath signal is half of the direct signal. The received data are combined by the amplitude and phase related to the propagation distance of two signals. In order to simulate the real measurement, a random signal is added to the received data.

In order to verify the effectiveness of the spectral extrapolation method, the received signal from 180 to 280 MHz is simulated as shown by the solid line in Fig. 3. The interval of frequency is 1 MHz. The received signal fluctuates due to the interference signals. The frequency domain signal is transformed to the time-domain response, which is shown by the solid line in Fig. 4. The bandwidth of 100 MHz corresponds to a range resolution of 3 m, which is almost equal to the distance between two signals, so it is hard to remove the multipath signal with a time gating.

Next, the frequency range of the received signal is extrapolated to 130–330 MHz using the maximum entropy spectral estimation algorithm, as shown by the dotted line in Fig. 3. The changed trend after extrapolation is consistent with the original frequency domain signal. The IFFT is used in the new frequency domain

https://doi.org/10.1017/S1759078718001241 Published online by Cambridge University Press

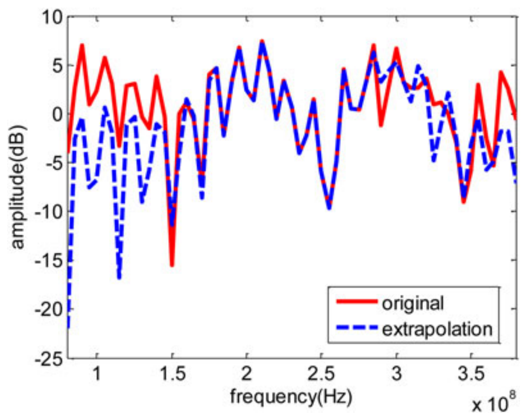

Fig. 6. The effective range of extrapolated data.

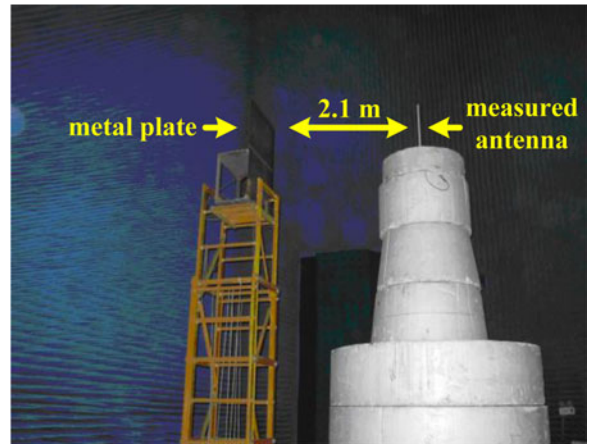

Fig. 8. Experimental photograph.

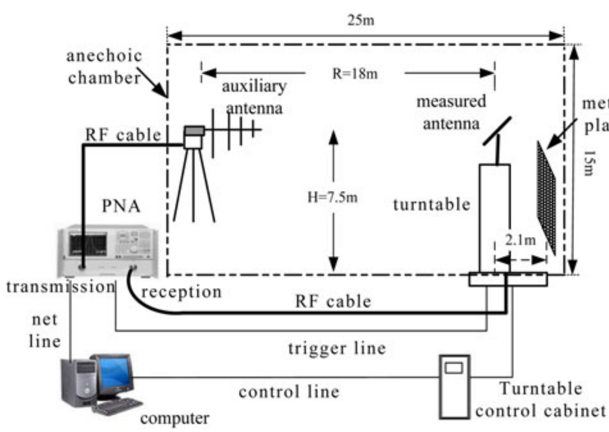

Fig. 7. Low-frequency antenna measurement with interference.

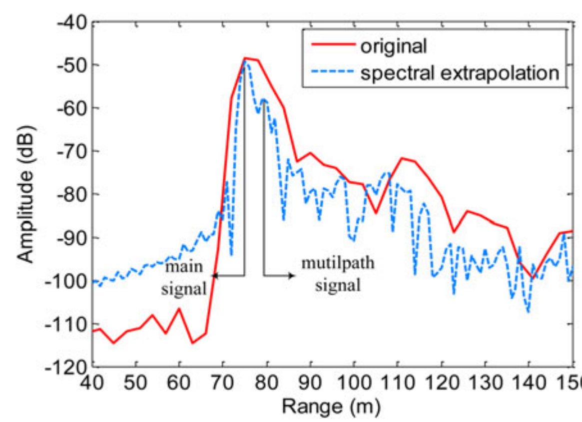

Fig. 9. The time-domain response of measurement and extrapolation.

signal, and the new time-domain curve is obtained as shown by the dotted line in Fig. 4. The time-domain resolution is enhanced doubly, and the corresponding range resolution also reaches 1.5 m. Then, we can see the direct signal and multipath signal clearly, so it is possible to use a time gating to remove the multipath signal.

In general, the model order p is not known in advance, and a large value needs to be selected at first and determine during recursion. As shown in Fig. 5, the error power decreases as the order increases. The appropriate order is selected when the error power is essentially constant. As can be seen from the figure, when the order is greater than six, the variation of error power is basically small, so the model order is six.

In order to investigate the effective range of extrapolated data, the received signal at 80–380 MHz is simulated, and then the signal from 180 to 280 MHz is intercepted to be extrapolated. The results of the extrapolated signal and original signal are shown in Fig. 6. It can be seen from the figure that most of the extrapolated data from 130 to 350 MHz have the same trend as the original data.

The experimental results

The low-frequency narrow-band antenna measurement system in an anechoic chamber is shown in Fig. 7. A vector network analyzer is used to transmit and receive stepped-frequency signals. The dipole antenna is placed on a turntable to measure the antenna directional pattern. A log-periodic antenna is used as the receiving antenna. Both the transmitted signal and the received signal are coherent signals and therefore the relative phase can be obtained.

The experimental photograph is shown in Fig. 8. The walls and ground of the anechoic chamber are covered by lots of absorbing material, whose reflectivity is approximately −30 dB at 500 MHz. A dipole antenna with the center frequency 350 MHz is measured. The frequency range of measurement is 300–400 MHz; the frequency interval is 1 MHz. The range of rotational angle is 360°; the angle interval is 1°. A metal plate is placed at the rear of the measured antenna, which is to simulate an interference signal. The distance between the metal plate and the dipole antenna is 2.1 m.

In order to verify the effectiveness of the method, an IFFT is applied to the original bandwidth, and the time-domain response is shown by the solid line in Fig. 9. As can be seen, the time-domain resolution is low and it is difficult to separate the multipath signal of the metal plate and the dipole antenna signal. In order to distinguish the multipath signal, the bandwidth is extended from 200 to 500 MHz using spectral extrapolation. The corresponding range-resolution is 1 m. The time-domain response after extrapolation is shown by the dashed line in Fig. 9. We can clearly see the dipole antenna signal and the multipath signal from the metal plate. The distance between them is about 4 m (two ways). Then a time gating is used to select the measured antenna signal accurately, which removes the multipath signal from the received signal.

Figure 10 shows the three unitary antenna patterns at 350 MHz. When the metal plate is near the antenna, the antenna

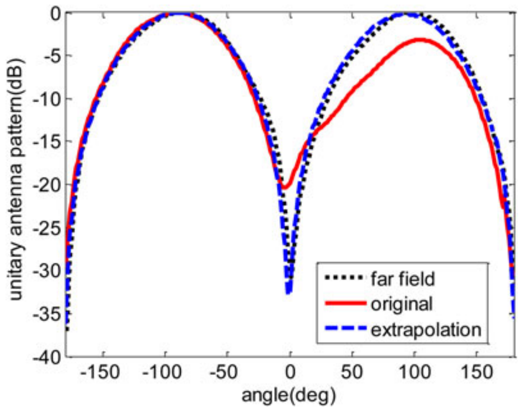

Fig. 10. The unitary antenna patterns

pattern is distorted. The main-side lobe is 3–5 dB lower than the measured far-field pattern, and the bottom of pattern is about −20 dB. The unsymmetrical disturbance of antenna is for the reason that the antenna was located outside of the rotation axis. After using the method, the multipath signal of the metal plate is mostly removed. The main-side lobe is <1 dB and the bottom of pattern is >−30 dB. The result almost coincides with the measured far-field pattern, which verifies the effectiveness of the method.

Conclusion

This paper presents a signal processing method to improve the measurement accuracy of low-frequency narrow-band antennas. The wideband signal is obtained by extrapolating the original band according to modern spectral estimation theory, the time-domain resolution is also improved after extrapolation; thereby the influence of the multipath signal is eliminated. The simulation and experiment show that the method shows good results. In the method, there are some suggestions for the extrapolated frequency domain range and the selection of model order p. First, if the extrapolated frequency domain range is too small, the time-domain resolution will not be improved obviously. If the extrapolated frequency domain range is too large, it will lead to distortion of time-domain response. We recommend that the frequency domain range after extrapolation is twice than the original bandwidth. Second, when the model order is increasing, the time-domain resolution will be improved. But if the model order continues to increase, the improved effect will not be obvious.

In the actual low-frequency narrow-band antenna measurement, the measured pattern often appears fluctuation. The method can be used to improve the result. Moreover, the method can be applied to higher frequency antenna measurement and used under indoor or outdoor conditions.

Acknowledgements. The authors thank the reviewers for their questions and suggestions. This work was supported by the National Natural Science Foundation of China (no. 61871323 and 61571368).

References

1. **Paonessa F, Virone G, Capello E, Addamo G, Peverini OA, Tascone R, Bolli P, Pupillo G, Monari M, Perini F, Rusticelli S, Lingua AM, Piras M, Aicardi I and Maschio P** (2016) VHF/UHF antenna pattern measurement with unmanned aerial vehicles. *IEEE Metrology for Aerospace*, Florence, Italy.
2. **Virone G, Lingua AM, Piras M, Cina A, Perini F, Monari J, Paonessa F, Peverini OA, Addamo G and Tascone R**, (2014) Antenna pattern verification system based on a micro unmanned aerial vehicle (UAV). *IEEE Antennas Wireless Propagation Letters* **13**, 169–172.
3. **Aubin J and Winebrand M** (2010) Side wall diffraction & optimal back wall design in elongated chambers for far–field antenna measurements at VHFUHF Frequencies. *Proceedings of IEEE Antennas and Propagation Society International Symposium*, Toronto, Canada.
4. **Yinusa KA and Eibert TF** (2013) A multi-probe antenna measurement technique with echo suppression capability. *IEEE Transactions on Antennas and Propagation* **61**, 5008–5016.
5. **Chou HT and Chou SJ** (2016) Multipath suppression for a 2-D far-field pattern in a hybrid antenna measurement facility using single-frequency data. *IEEE Transactions on Antennas and Propagation* **64**, 4083–4087.
6. **González-Blanco P and Sierra-Castañer M** (2016) Time filtering techniques for echo reduction in antenna measurements. *Proceedings of European Conference on Antennas and Propagation*, Davos, Switzerland.
7. **Foged LJ, Scialacqua L, Mioc F, Saccardi F, Iversen PO, Shmidov L, Braun R, Araque Quijano JL and Vecchi G** (2013) Echo suppression by spatial-filtering techniques in advanced planar and spherical near-field antenna measurements. *IEEE Antennas Propagation Magazine* **55**, 235–242.
8. **Cano-Fácila FJ, Burgos S, Martín F and Sierra-Castaner M** (2011) New reflection suppression method in antenna measurement systems based on diagnostic techniques. *IEEE Transactions on Antennas and Propagation* **59**, 941–949.
9. **Foged LJ, Scialacqua L, Saccardi F, Mioc F, Iversen PO, Shmidov L, Braun R, Araque Quijano JL and Vecchi G** (2013) Comparison of echo suppression techniques in near field antenna measurements applications. *Proceedings of European Conference on Antennas and Propagation*, Gothenburg, Sweden.
10. **Mauermayer RAM and Eibert TF** (2016) Time gating based on sparse time domain signal reconstruction from limited frequency domain information. *Symposium of the Antenna Measurement Techniques Association*, Texas, USA.
11. **Le Fur G, Cano-Facila F and Saccardi F** (2014) Improvement of antenna measurement results at low frequencies by using post-processing techniques. *Proceedings of European Conference on Antennas and Propagation*, Hague, The Netherlands.
12. **Gregson SF, Newell AC and Hindman GE** (2013) Behavior of orthogonal wave functions and the correction of antenna measurements taken in non-anechoic environments. *Antennas and Propagation Conference*, Loughborough, UK.
13. **Kurokawa S, Hirose M and Ameya M** (2015) Precision antenna measurement using optical fiber link technologies. *IEEE Conference on Antenna Measurements and Applications*, Chiang Mai, Thailand.
14. **Li HJ, Liu TY and Leou JL** (2001) Antenna measurements in the presence of multipath waves. *Progress In Electromagnetics Research* **30**, 157–178.
15. **Ortigueira MD** (2014) On the recursive solution to the normal equations: some other results. *IEEE Signal Processing Magazine* **31**, 140–142.

C. F. Hu received his B.Sc. in 2004 and M.Sc. in 2007 both from Northwestern Polytechnical University, and obtained his Ph.D. from Northwestern Polytechnical University in 2010. Now he is a vice professor in Science and Technology on UAV Laboratory, Northwestern Polytechnical University. His research interests include antenna measurement and radar imaging and microwave remote sensing.

N. J. Li received his B.Sc. in 1998 and M.Sc. in 2001 both from Northwestern Polytechnical University, and obtained his Ph.D. from Northwestern Polytechnical University in 2006. Now he is a vice professor in Science and Technology on UAV Laboratory, Northwestern Polytechnical University. His research interests include antenna measurement and radar imaging and microwave remote sensing.